

Electronic transport through a quantum dot with a magnetic impurity using the equation of motion

Mugurel Tolea

*National Institute of Materials Physics,
POBox MG7, Bucharest-Magurele, Romania and
Institute of Molecular Physics, Polish Academy of Science,
ul. M. Smoluchowskiego 17, 60-179 Poznań, Poland*

Bogdan R. Bulka

*Institute of Molecular Physics, Polish Academy of Science,
ul. M. Smoluchowskiego 17, 60-179 Poznań, Poland*

Abstract

We study the electronic transport through a quantum dot containing a magnetic impurity, using the equation of motion approach. For temperatures above the Kondo temperature, an analytical solution can be obtained for the conductance, occupancy and the spin-spin correlator. The spins are weakly correlated when both singlet and triplet levels are below the Fermi energy, allowing for developing of the Kondo effect in a low temperature. The height of the conductance peaks corresponding to the singlet and triplet states depends on the ratio J/Γ (an exchange parameter versus a coupling strength with the leads), fundamentally different from the two-electrons spin-scattering picture. We also compute the phase evolution for the single-electron Green function and find that it has a specific dip at the excited state position. For low temperatures, we demonstrate the formation of three Kondo peaks: one at the Fermi energy and two side peaks, at a distance corresponding to the singlet-triplet level spacing. An analytical formula is found that associates the existence of the central peak (the only one important for large exchange parameter) with the value of the spin-spin correlator, the Kondo effect being suppressed for strong antiferromagnetic correlations.

I. INTRODUCTION

Quantum dots (QD) are promising systems for nano-technology because their quantum-mechanical parameters are easy to control. Motivated, in part, by the recent developing in the field of magnetic semiconductors [1], or by the spintronic advances, theorists and experimentalists have started to address also the problem of Quantum Dots with magnetic impurities [2, 3, 4, 5]. Sometimes, the role of the impurity is played by another quantum dot with odd occupancy [6], but also, as in a recent experiment [5], the impurity can be a transitional magnetic atom (Co). The splitting of the Kondo peak was attributed by the authors to the indirect RKKY interaction [7, 8]. We believe that a central peak would have also been present for a much lower temperature. Govorov [2] studied theoretically the spectrum and the response to optical excitations of an InGaAs/GaAs quantum dot with a single Mn impurity. Recently, Murthy [3] also addressed the problem of a large quantum dot with a magnetic impurity. In his spectral calculations, the Kondo effect originates in the dot itself. A suppression of this effect is predicted in conditions of strong antiferromagnetic coupling between the magnetic impurity and the electrons in the dot.

In the present paper we are also interested in the Kondo resonance, but in a different system: a small quantum dot for which the Kondo effect is originating in the dot-leads correlations, following the usual experimental set-up [9, 10]. Moreover, a magnetic impurity will be acting on the dot's electrons through an exchange interaction. We would like to consider spin-flip processes on the impurity and their detection by the current flowing through the QD, both in high and low temperature regimes. To our knowledge, the problem was not considered yet. In spectral terms, the flip of the impurity spin is associated with singlet-triplet excitations. We study the Kondo resonance, which for the singlet-triplet level structure leads to a peak in the local density of states at the Fermi energy E_F and two side peaks (at a distance corresponding to the singlet-triplet level-spacing). The peak at E_F will not be present in the case when only the singlet state is below E_F . This is because the singlet state implies strong antiferromagnetic entanglement (between the electron in the dot and the impurity) that naturally inhibits the Kondo effect (originated, on the contrary, in the dot-leads correlations). But the suppression of Kondo also happens because of the reduction (in our case disappearing) of the ground state degeneracy. The equation of motion method will allow us to obtain an analytical expression directly relating the existence of the peak at

E_F with the value of the spin-spin correlator. It is clear that there is a strong motivation in calculating the spin-spin correlator, and this will be a key element in our interpretations.

Apart for the Kondo regime, we shall also analyze the regime of temperatures higher than T_K (this will be done first, as the problem allows for fully analytical results), where the dynamics of electrons still show clear correlations effects. For instance, the peaks in conductance that correspond to excited states depend strongly on the coupling with the leads and are absent for low coupling. The height of the peaks corresponding to ground states depends weakly on the coupling to the leads. This differs fundamentally from the two-electrons spin scattering picture (recently applied in [11] to describe the 0.7 anomaly in quantum wires) when the Fermi sea is neglected and where the triplet peak is always three times higher than the singlet peak (due to the tree-fold degeneracy of the triplet state). The excited states also have a distinct signature on the phase evolution, namely a dip of considerable amplitude, that can be detected experimentally even when the transmittance on the excited states is very low.

The paper is organized as follows: in the Section II we present details of our model and in Section III we explain our method for calculations of the conductance and give the solution in the high temperature regime. The conductance through ground and excited states is analyzed, together with values of the occupancy, the spin-spin correlator and the phase evolution. As an example, we will find that the spin-spin correlator is reduced when both singlet and triplet levels are below the Fermi energy, in a wide range of a gate potential, permitting for the developing of a robust Kondo effect, as it was suggested in previous papers [12, 13] (for a double-dot system). The section IV is devoted to low temperatures and the Kondo regime, with the formation of three Kondo peaks in the local DOS: at E_F and $E_F \pm J$. For a large exchange coupling J , only the peak at E_F is of interest and we show that it exists only if the triplet state is below the Fermi energy. Otherwise, if only the singlet energy is below E_F , the high (in module) negative value of the spin-spin correlator prevents the formation of the Kondo resonance. The section V contains concluding remarks. For completeness the spectrum of the system is presented in the Appendix.

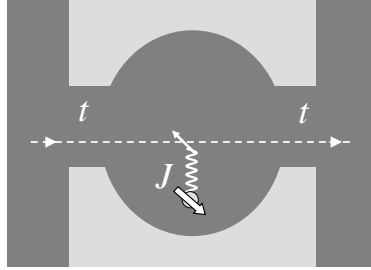


FIG. 1: Scheme of a quantum dot coupled to ideal leads through tunnelling barriers t . A magnetic impurity interacts with electrons in the dot through an exchange coupling J .

II. MODEL OF A QUANTUM DOT WITH A MAGNETIC IMPURITY

The considered system of the QD with a magnetic impurity is presented in Fig. 1. Conduction electrons passing through the QD interact with accumulated electrons leading to the Kondo resonance in low temperatures. Supplementary, a magnetic impurity is connected to the electrons in the QD by the exchange coupling J . The Hamiltonian corresponding to our model is written as

$$H = \sum_{k,\sigma,\alpha} \epsilon_k c_{k\sigma,\alpha}^\dagger c_{k\sigma,\alpha} + \epsilon_0 \sum_{\sigma} c_{0\sigma}^\dagger c_{0\sigma} + U c_{0\uparrow}^\dagger c_{0\uparrow} c_{0\downarrow}^\dagger c_{0\downarrow} + J \vec{s} \cdot \vec{S} + \sum_{k,\sigma,\alpha} t_{\alpha} (c_{0\sigma}^\dagger c_{k\sigma,\alpha} + h.c.) , \quad (1)$$

where the first term represents the electrons in the lead α , the second term stands for the up-most electronic level ϵ_0 in the dot. The the third and the fourth terms describe interactions: Coulombic interaction of electrons with the opposite spin orientation at the level ϵ_0 and exchange interactions with the magnetic impurity. Here, \vec{s} is the spin operator for electrons at the level ϵ_0 , whereas \vec{S} denotes the spin operator at the magnetic impurity. It is imposed a single occupancy at the impurity $d_{\uparrow}^\dagger d_{\uparrow} + d_{\downarrow}^\dagger d_{\downarrow} = 1$ and the the spin $S = 1/2$. Therefore, $S^z = 1/2(d_{\uparrow}^\dagger d_{\uparrow} - d_{\downarrow}^\dagger d_{\downarrow})$, $S^+ = d_{\uparrow}^\dagger d_{\downarrow}$, $S^- = d_{\downarrow}^\dagger d_{\uparrow}$, and the exchange term between the impurity and the spin of the electron localized at the QD can be written as

$$J \vec{s} \cdot \vec{S} = \frac{1}{2} J (c_{0\uparrow}^\dagger c_{0\uparrow} - c_{0\downarrow}^\dagger c_{0\downarrow}) S^z + \frac{1}{2} J c_{0\uparrow}^\dagger c_{0\downarrow} S^- + \frac{1}{2} J c_{0\downarrow}^\dagger c_{0\uparrow} S^+ . \quad (2)$$

The last term in the Hamiltonian (1) corresponds to the coupling between the quantum dot and the leads. Without losing generality we consider the symmetric case $t_L = t_R = t$, in which it is not necessary to further write the lead index α for the $c_{k\sigma}$ operators. The summation over α will not be explicitly written, but it should be understood.

We shall focus, in this paper, on the physical predictions at zero magnetic field. However, the case in which the main effect of the magnetic field is on the orbital motion of electrons [14] (so the field induces variations of J only and the Zeeman energy can be neglected) is captured.

For our model (1) we choose the equation of motion method in order to calculate the conductance and other physical quantities. The method allows to get analytical results and it gives correct description of the Kondo physics [15, 16, 17, 18]. Details of the approach are presented in the next section.

III. EQUATION OF MOTION - THE HIGH TEMPERATURE APPROXIMATION

Current measurements are the main experimental tool for investigating quantum dots. The current flow is a non-equilibrium situation and one of the existing theoretical methods to address it is the non-equilibrium Green's functions technique. In our particular case (the single-site dot with a symmetric coupling) the current can be written [19]

$$j = \frac{e}{h} \Gamma \int d\omega [f_L(\omega) - f_R(\omega)] (-\text{Im} \langle \langle c_{0\sigma} | c_{0\sigma}^\dagger \rangle \rangle_\omega), \quad (3)$$

where $\Gamma = 2\pi t^2 \rho$, $\rho = 1/2D$ is the DOS at the Fermi level for the square band of the half-width D taken as unity, and $\langle \langle c_{0\sigma} | c_{0\sigma}^\dagger \rangle \rangle_\omega$ is the retarded Green function.

The equation of motion (EOM) for the energy dependent retarded Green function is

$$\omega \langle \langle A | B \rangle \rangle_\omega = \langle \{A, B\} \rangle + \langle \langle [A, H] | B \rangle \rangle_\omega, \quad (4)$$

where $\langle \{A, B\} \rangle$ is the average value of the anticommutator between the fermionic operators A and B. Generally, the energy dependence of the Green functions will not be explicitly written. Whenever necessary, the averages will be expressed by making use of the fluctuation-dissipation theorem $\langle AB \rangle = -(1/\pi) \int d\omega f(\omega) \text{Im} \langle \langle B | A \rangle \rangle$.

We write the equations for the Quantum Dot Green functions. It is convenient to use the compact spin notation for the localized electrons, since there are always either none or

two "d" operators (grouped to form a spin operator).

$$\begin{aligned}
(\omega - \epsilon_0) \langle \langle c_{0\uparrow} | c_{0\uparrow}^\dagger \rangle \rangle &= 1 + U \langle \langle c_{0\uparrow} c_{0\downarrow}^\dagger c_{0\downarrow} | c_{0\uparrow}^\dagger \rangle \rangle + \frac{1}{2} J \langle \langle c_{0\uparrow} S^z | c_{0\uparrow}^\dagger \rangle \rangle \\
&\quad + \frac{1}{2} J \langle \langle c_{0\downarrow} S^- | c_{0\uparrow}^\dagger \rangle \rangle + t \sum_k \langle \langle c_{k\uparrow} | c_{0\uparrow}^\dagger \rangle \rangle \\
(\omega - \epsilon_0) \langle \langle c_{0\uparrow} S^z | c_{0\uparrow}^\dagger \rangle \rangle &= \langle S^z \rangle + \frac{1}{8} J \langle \langle c_{0\uparrow} | c_{0\uparrow}^\dagger \rangle \rangle + U \langle \langle c_{0\uparrow} c_{0\downarrow}^\dagger c_{0\downarrow} S^z | c_{0\uparrow}^\dagger \rangle \rangle \\
&\quad - \frac{1}{4} J \langle \langle c_{0\downarrow} S^- | c_{0\uparrow}^\dagger \rangle \rangle + \frac{1}{2} J \langle \langle c_{0\downarrow} c_{0\uparrow}^\dagger c_{0\uparrow} S^- | c_{0\uparrow}^\dagger \rangle \rangle \\
&\quad + t \sum_k \langle \langle c_{k\uparrow} S^z | c_{0\uparrow}^\dagger \rangle \rangle \\
(\omega - \epsilon_0 + \frac{1}{4} J) \langle \langle c_{0\downarrow} S^- | c_{0\uparrow}^\dagger \rangle \rangle &= \frac{1}{4} J \langle \langle c_{0\uparrow} | c_{0\uparrow}^\dagger \rangle \rangle + (U + \frac{1}{2} J) \langle \langle c_{0\downarrow} c_{0\uparrow}^\dagger c_{0\uparrow} S^- | c_{0\uparrow}^\dagger \rangle \rangle \\
&\quad - \frac{1}{2} J \langle \langle c_{0\uparrow} S^z | c_{0\uparrow}^\dagger \rangle \rangle + J \langle \langle c_{0\uparrow} c_{0\downarrow}^\dagger c_{0\downarrow} S^z | c_{0\uparrow}^\dagger \rangle \rangle \\
&\quad + t \sum_k \langle \langle c_{k\downarrow} S^- | c_{0\uparrow}^\dagger \rangle \rangle \\
(\omega - \epsilon_0 - U) \langle \langle c_{0\uparrow} c_{0\downarrow}^\dagger c_{0\downarrow} | c_{0\uparrow}^\dagger \rangle \rangle &= \langle c_{0\downarrow}^\dagger c_{0\downarrow} \rangle + \frac{1}{2} J \langle \langle c_{0\uparrow} c_{0\downarrow}^\dagger c_{0\downarrow} S^z | c_{0\uparrow}^\dagger \rangle \rangle + \frac{1}{2} J \langle \langle c_{0\downarrow} c_{0\uparrow}^\dagger c_{0\uparrow} S^- | c_{0\uparrow}^\dagger \rangle \rangle \\
&\quad + t \sum_k \langle \langle c_{k\uparrow} c_{0\downarrow}^\dagger c_{0\downarrow} | c_{0\uparrow}^\dagger \rangle \rangle - t \sum_k \langle \langle c_{0\uparrow} c_{k\downarrow}^\dagger c_{0\downarrow} | c_{0\uparrow}^\dagger \rangle \rangle \\
&\quad + t \sum_k \langle \langle c_{0\uparrow} c_{0\downarrow}^\dagger c_{k\downarrow} | c_{0\uparrow}^\dagger \rangle \rangle \\
(\omega - \epsilon_0 - U) \langle \langle c_{0\uparrow} c_{0\downarrow}^\dagger c_{0\downarrow} S^z | c_{0\uparrow}^\dagger \rangle \rangle &= \langle c_{0\downarrow}^\dagger c_{0\downarrow} S^z \rangle + \frac{1}{8} J \langle \langle c_{0\uparrow} c_{0\downarrow}^\dagger c_{0\downarrow} | c_{0\uparrow}^\dagger \rangle \rangle + \frac{1}{4} J \langle \langle c_{0\downarrow} c_{0\uparrow}^\dagger c_{0\uparrow} S^- | c_{0\uparrow}^\dagger \rangle \rangle \\
&\quad + t \sum_k \langle \langle c_{k\uparrow} c_{0\downarrow}^\dagger c_{0\downarrow} S^z | c_{0\uparrow}^\dagger \rangle \rangle - t \sum_k \langle \langle c_{0\uparrow} c_{k\downarrow}^\dagger c_{0\downarrow} S^z | c_{0\uparrow}^\dagger \rangle \rangle \\
&\quad + t \sum_k \langle \langle c_{0\uparrow} c_{0\downarrow}^\dagger c_{k\downarrow} S^z | c_{0\uparrow}^\dagger \rangle \rangle \\
(\omega - \epsilon_0 - \frac{1}{4} J - U) \langle \langle c_{0\downarrow} c_{0\uparrow}^\dagger c_{0\uparrow} S^- | c_{0\uparrow}^\dagger \rangle \rangle &= -\langle c_{0\uparrow}^\dagger c_{0\downarrow} S^- \rangle + \frac{1}{4} J \langle \langle c_{0\uparrow} c_{0\downarrow}^\dagger c_{0\downarrow} | c_{0\uparrow}^\dagger \rangle \rangle + \frac{1}{2} J \langle \langle c_{0\uparrow} c_{0\downarrow}^\dagger c_{0\downarrow} S^z | c_{0\uparrow}^\dagger \rangle \rangle \\
&\quad + t \sum_k \langle \langle c_{k\downarrow} c_{0\uparrow}^\dagger c_{0\uparrow} S^- | c_{0\uparrow}^\dagger \rangle \rangle - t \sum_k \langle \langle c_{0\downarrow} c_{k\uparrow}^\dagger c_{0\uparrow} S^- | c_{0\uparrow}^\dagger \rangle \rangle \\
&\quad + t \sum_k \langle \langle c_{0\downarrow} c_{0\uparrow}^\dagger c_{k\uparrow} S^- | c_{0\uparrow}^\dagger \rangle \rangle
\end{aligned} \tag{5}$$

In the absence of a magnetic field, one can consider $\langle S^z \rangle = 0$, $\langle c_{0\downarrow}^\dagger c_{0\downarrow} \rangle = \langle c_{0\uparrow}^\dagger c_{0\uparrow} \rangle$ and $\langle c_{0\downarrow}^\dagger c_{0\downarrow} S^z \rangle = -\frac{1}{2} \langle c_{0\uparrow}^\dagger c_{0\downarrow} S^- \rangle = -\frac{1}{3} \langle \vec{s} \cdot \vec{S} \rangle$, $(S^z)^2 = \frac{1}{4}$ (see also [20] for some details on how the property $d_\uparrow^\dagger d_\uparrow + d_\downarrow^\dagger d_\downarrow = 1$ was used). In the following, it is needed to express the Green functions that have a c_k operator from the leads. First, we find easily

$$t \sum_k \langle \langle c_{k\uparrow} | c_{0\uparrow}^\dagger \rangle \rangle = \sum_k \frac{t^2}{\omega - \epsilon_k} \langle \langle c_{0\uparrow} | c_{0\uparrow}^\dagger \rangle \rangle \approx -2i\pi t^2 \rho \langle \langle c_{0\uparrow} | c_{0\uparrow}^\dagger \rangle \rangle \tag{6}$$

The last relation was obtained by transforming the sum over k in integral and keeping only the imaginary part of this integral (a factor two appears because there are two leads). This is the typical "square band" approximation [21]. We point out that this means the adding of a imaginary part $\Gamma = 2\pi t^2 \rho$ to the energy ϵ_0 in the first of Eqs.(5).

Next we make the following approximation

$$t \sum_k \langle\langle c_{k,\sigma} A | c_{0,\sigma}^\dagger \rangle\rangle \approx -i\Gamma \langle\langle c_{0,\sigma} A | c_{0,\sigma}^\dagger \rangle\rangle \quad (7)$$

which is the same as in [12, 13]. We can call this high temperature approximation. In this approximation the coupling to the leads is considered in the lowest order, meaning that we shall simply add a imaginary part Γ (a "linewidth") to ϵ_0 , in all Eqs. (5), although is exact only for the first equation.

It is interesting to mention here that, since the Hamiltonian (1) conserves the total spin (unlike the Hamiltonian used in [22]), the flip Green function $\langle\langle c_{0\sigma} | c_{0\bar{\sigma}}^\dagger \rangle\rangle$ will vanish, and non-flip Green functions carry all the relevant information for the transport (although intermediate flip processes are present and accordingly taken into account). Zhang et al. [22] added a one-body spin-flip term (accounting for the spin-orbit interaction) to the Anderson Hamiltonian and also predicted three Kondo peaks in the presence of parallel-magnetized ferromagnetic leads.

On the other hand we shall take into account all many-body correlation within the Quantum Dot. It means that no approximations or decouplings were made on the higher order Green functions that refer to the dot only [those that appear on the left side of Eqs.(5)]. This approach gives reliable results for high temperatures and represents an easy way to get analytic description of the excited states in the dot. We shall give further details in the interpretation of the results. In this approximation, the transport properties of the system completely result from the set of six equations of motion Eqs.(5).

In order to solve a set of Eqs.(5), we first perform a spectral decomposition of the Green functions. It means that any Green functions is written as a combination of the simple fractions with some coefficients expressed by the correlators $\langle c_{0\uparrow}^\dagger c_{0\uparrow} \rangle$ and $\langle c_{0\uparrow}^\dagger c_{0\uparrow} S^z \rangle$. Next, the correlators are determined by means of the appropriate Green functions $\langle c_{0\uparrow}^\dagger c_{0\uparrow} \rangle = -(1/\pi) \int d\omega f(\omega) \text{Im} \langle\langle c_{0\uparrow} | c_{0\uparrow}^\dagger \rangle\rangle$ and $\langle c_{0\uparrow}^\dagger c_{0\uparrow} S^z \rangle = -(1/\pi) \int d\omega f(\omega) \text{Im} \langle\langle c_{0\uparrow} S^z | c_{0\uparrow}^\dagger \rangle\rangle$. The integrals mentioned can be expressed by *digamma* functions (as it results when the product between the Fermi function and a simple fraction is integrated - see [23]; also, at *zero* tem-

perature, the integrals become arctan). Thus we have a set of linear equations, which has to be solved. As we said, this is an accurate solution at high temperatures. However, at the temperature $T = 0$ the solution is more easy to get analytically and it contains most of the relevant physics. Finite temperatures add basically just a smearing of the resonances, as the temperature becomes comparable with the broadening (see [12] for all details of the effects of finite temperature). While the temperature effect is rather trivial, the effects of correlations on the dot (our main interest here) are not, so we make some simplifications for the benefit of a more clear exposure. Also we can say that there exists a (rather large) range of temperatures that are too high for the developing of the Kondo correlations but can still be approximated with *zero* from the point of view of the charge fluctuations (that have a bigger broadening than $k_B T$).

Coming back to considerations of the spin correlations, we say that, when $J > 0$ the singlet is lower in energy and represents the ground state (SGS) for single occupancy of the "0" orbital. On the contrary, when $J < 0$ we have the triplet state as the ground state (TGS) (see the Appendix). Excited states are also seen in the conductance, but they do not change the electronic occupancy, as the electron was already added on the ground state. However, when such an excited state becomes available for transport (goes below E_F) this has an influence on the value of the spin-spin correlator, as we shall see. The existence of such excited states has been experimentally proven and measured (e.g. the recent experiment of Rogge et all. [24]), and they are of particular importance when explaining the physics of nonequilibrium conductance, and also for the Kondo effect, case in which they give raise to a multiple-peak structure in the vicinity of the Fermi energy (we address this problem in the next section).

Since we are focusing on understanding of the new correlations introduced, the conductance is analyzed close the equilibrium. Based on the current formula Eq.(3), the conductance can be written

$$\mathcal{G} = \frac{e^2}{h} \Gamma \int d\omega \left(-\frac{\partial f(\omega)}{\partial \omega} \right) \text{Im} \langle \langle c_{0\uparrow} | c_{0\uparrow}^\dagger \rangle \rangle_\omega . \quad (8)$$

For $k_B T \ll \Gamma$ (i.e. low temperature limit) one has simply $\mathcal{G} = -(e^2/h) \Gamma \text{Im} \langle \langle c_{0\uparrow} | c_{0\uparrow}^\dagger \rangle \rangle_{E_F}$. We give some plots for the conductance and the correlators (that completely determine the problem) in Fig.2. The first and the last peak in each graph correspond to ground states (on which the occupation number varies). The plots are both for *positive* J (Fig.2a) and *negative*

J (Fig.2b), in each case the positions for the singlet and triplet resonances are indicated by vertical lines. Throughout the paper we assume the position of the Fermi level $E_F = 0$.

The antiferromagnetic coupling favors the singlet state. The spin-spin correlator is then negative, for the case presented in the upper panel of Fig.2a, reaching the minimal value -0.7 . Accordingly, the length of the total momentum $\langle \vec{S}_{tot}^2 \rangle = \langle \vec{s}^2 \rangle + 2\langle \vec{s} \cdot \vec{S} \rangle + \langle \vec{S}^2 \rangle$ is reduced to 0.1 , i.e. it is almost compensated. The minimal value reached by $\langle \vec{s} \cdot \vec{S} \rangle$ does not directly depend neither on the strength of the exchange interaction J , nor on the coupling Γ (that is usually easier to vary in experiments), but on the ratio J/Γ (with the values 10 , 2.5 and 1 in Fig.2a). For the cases presented in two lower panels in Fig.2a, the ratio J/Γ is smaller and the singlet and the triplet states overlap, which results in reduction of the antiferromagnetic coupling. When the triplet state also gets below Fermi energy, the value of the spin-spin correlator increases, which is associated with the fact that the triplet state favors ferromagnetic coupling. This increase of the spin-spin correlator will go on until the middle point between the two group of peaks is met. For the upper panel in Fig.2a the maximal value of $\langle \vec{s} \cdot \vec{S} \rangle \approx -0.1$, which means $\langle \vec{S}_{tot}^2 \rangle \approx 1.3$ close to $3/2$ - the value of the magnetic moment for two free $S = 1/2$ spins. The evolution of all quantities in Fig.2 from the middle point result from an electron-hole symmetry, so a separate analysis is not necessary. This reduced value of the spin-spin correlator, for a rather large range of parameters, is an important result, that suggests a possible developing of the Kondo effect, that may be captured for a more accurate, non-perturbative decoupling scheme. The next section will prove that indeed this is the case.

The evolution of the correlators for the ferromagnetic coupling (presented in Fig.2b) can be explained in the same way: when E_F crosses the T state (that is lowest in energy for $J < 0$) the spin-spin correlator has positive values reaching respectively (from upper to lower panel): 0.22 , 0.18 and 0.1 . The total magnetic moment reaches up to 1.94 , 1.86 and 1.7 , respectively. For each of the three situations, the spin-spin correlator and the total moment begin to decrease when the singlet also gets below E_F , until the middle of the band is reached.

In the following, we shall discuss the heights of the conductance peaks corresponding to the singlet and triplet peaks. For $T = 0$ and in the limit $U \rightarrow \infty$, we get an analytical

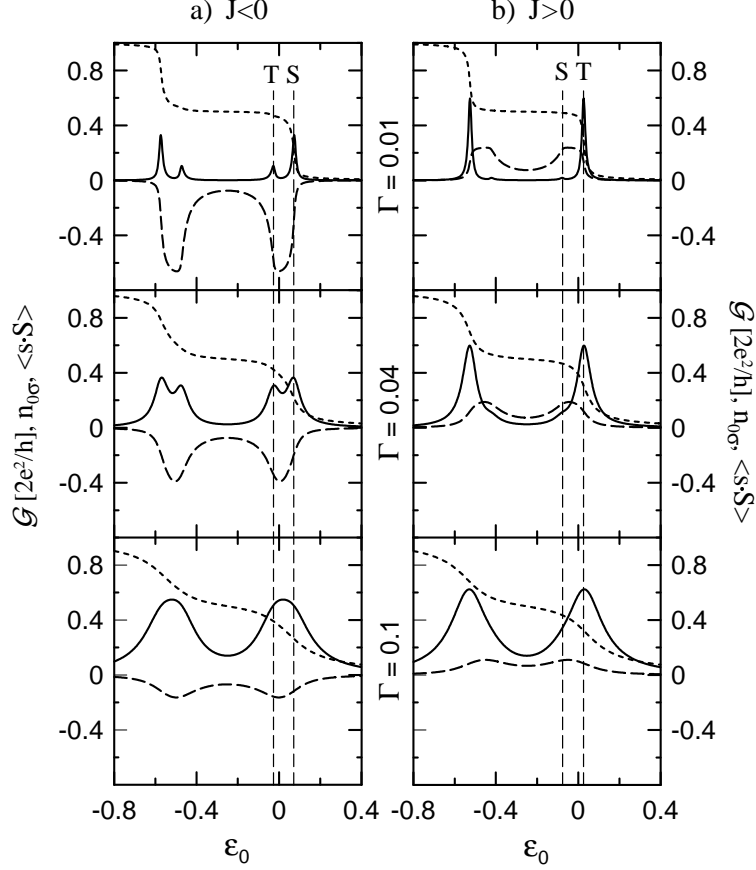


FIG. 2: Conductance \mathcal{G} (solid lines), the spin-spin correlator $\langle \vec{s} \cdot \vec{S} \rangle$ (dashed) and the average dot occupancy $\langle c_{0\sigma}^\dagger c_{0\sigma} \rangle$ per spin (dotted) plotted as a function of the position of the dot level ϵ_0 , for different couplings with the leads $\Gamma = 0.01, 0.04$ and 0.1 . For the column a) $J = 0.1$ and the system is in the Singlet Ground State; the column b) corresponds to the ferromagnetic coupling $J = -0.1$ when the system has the Triplet Ground State. The vertical lines indicate the position of the Singlet and Triplet levels. Notice that the height of the peak corresponding to the exciting state (the triplet in case a and the singlet in case b) strongly depends on the coupling with the leads, unlike the peaks corresponding to ground states. Also, in the central part of each graph, when both S and T are below E_F (but the levels for double occupancy are not) the module of the spin-spin correlator is low. In all graphs $U = 0.5$.

solution for the conductance

$$\mathcal{G} = \mathcal{G}_S + \mathcal{G}_T = R_S \frac{1 + 2\phi_T}{2(3 + 4\phi_S - 4\phi_S\phi_T)} + R_T \frac{3(1 + 2\phi_S)}{2(3 + 4\phi_S - 4\phi_S\phi_T)}, \quad (9)$$

where $R_S = (2e^2/h) \times \Gamma^2 / [\Gamma^2 + (E_F - \epsilon_0 + 3J/4)^2]$ and $R_T = (2e^2/h) \times \Gamma^2 / [\Gamma^2 + (E_F - \epsilon_0 - J/4)^2]$ corresponds to the resonant conductance through the singlet and the triplet level,

respectively, $\phi_S = \arctan[(\epsilon_0 - E_F - 3J/4)/\Gamma]/\pi$ and $\phi_T = \arctan[(\epsilon_0 - E_F + J/4)/\Gamma]/\pi$. This formula is accurate when the peaks are well separated. The general solution for the conductance \mathcal{G} (for any U) is not much more complicated, although a little lengthy. \mathcal{G} contains then also the other two resonances corresponding to the adding of the second electron. These resonances peaks are symmetric with the first two peaks (due to electron-hole symmetry), which can be seen in Fig.2, where the plots are for the general formula.

The formula (9) allows us to estimate the ratio between the heights of the conductance for the singlet and triplet peaks. This ratio is not $1/3$, as would be expected for an asymptotically free electron scattered on a bound electron in the QD considered by Rejec et al. [11]. Their problem is analogous to the electron collision with a hydrogen atom (see [25]). In such a case, exchange processes are taken into account and all relevant physics is comparison between the incident and the resonant energies. By averaging all possible scattering processes, the height of the singlet and triplet peaks will be proportional with their degeneracy resulting the $1/3$ peak height ratio. Such physics is successfully exploited in [11] to give an explanation to the 0.7 anomaly in quantum wires. The authors describe the scattering in the natural singlet/triplet base (the same is done in [4], where the scattering processes are individually analyzed).

The picture is different for our model, where the electrodes are considered as a Fermi sea and electronic correlations are taken into account. The electronic transport is usually due to local charge fluctuations, in which a number of electrons changes $n \leftrightarrow (n \pm 1)$. Transport through excited states can be explained by the fluctuations of the distribution of charge on the available levels in the dot. The conductance peak corresponding to the ground state is usually higher, no matter whether it is triplet or singlet. The difference results from the charge accumulation and the Coulomb blockade effect. The parameter that determines the peak height ratio is J/Γ .

We notice that in Eq.(9) the parameter ϕ_S (ϕ_T) vanishes at the singlet (triplet) resonant level, and therefore, one can straightforward calculate the ratio of the conductance peaks

$$\frac{\max[\mathcal{G}_S]}{\max[\mathcal{G}_T]} = \frac{[1 + \frac{2}{\pi} \arctan(\frac{J}{\Gamma})][3 - \frac{4}{\pi} \arctan(\frac{J}{\Gamma})]}{9[1 - \frac{2}{\pi} \arctan(\frac{J}{\Gamma})]} \quad (10)$$

For the situations in Fig.2 one gets the following singlet/triplet conductance ratios: 3.82 , 1.19 , 0.66 for the column a) and 0.02 , 0.07 , 0.14 for the column b) (from top to bottom), so when the singlet is excited state it becomes very weakly seen in transport. Moreover, in

this last case, when the coupling is large enough for the singlet peak to be observed clearly, it also happens that the overlap with the triplet peak becomes dominant (lower two panels in Fig.2b). In the large J limit and for $J > 0$ (the singlet ground state), the above ratio goes to *infinity* and the triplet peak disappears. For the ferromagnetic coupling and $|J| \gg \Gamma$ we have opposite situation - the singlet states disappears and only the peak corresponding the triplet ground state is visible. This means that when the coupling is very weak (with respect to, let's say, the energy level spacing), only the resonances corresponding to ground states are seen in transport and those corresponding to excited states are totally absent. Such a low-coupling case is seen in the upper plots of Fig.2. It is important to point here that, although the conductance hardly feels the excited states (in the low-coupling regime), the effect on the value of the spin-spin correlator is significant. The other limit case is when $\Gamma \gg J$. Then the ratio (10) is again 1/3, like in the noninteracting case, but the two peaks are no longer well separated (the two lower plots in Fig.2). In such case of strong coupling with the leads, when the singlet and triplet states simultaneously participate in transport, the spin-spin correlator has low values. We can also observe in Fig.2 that, due to its natural three-fold degeneracy, the excited triplet state (column a) is much better seen then the excited singlet state (column b).

Our formalism allows also to analyze the evolution of the phase for the single-electron Green function, defined as

$$\Phi = \arctan \left[\frac{\text{Im} \langle \langle c_{0\sigma} | c_{0\sigma}^\dagger \rangle \rangle_{\omega=E_F}}{\text{Re} \langle \langle c_{0\sigma} | c_{0\sigma}^\dagger \rangle \rangle_{\omega=E_F}} \right]. \quad (11)$$

The phase problem is interesting in mesoscopic physics [26] and it can be measured experimentally when the phase-lapse effect appears [27, 28]. The principle of the measurement uses an interference process, which has been realized by inserting the quantum dot - for which the phase is measured - in one arm of an Aharonov-Bohm interferometer. The phase of the dot is then extracted from the phase of the Aharonov-Bohm oscillations seen in the conductance. For simplicity, we shall discuss here only the situations like the upper panel in Fig2a, when the singlet and triplet peaks are well-separated (but the conclusions are universal). One could naively expect that the phase grows with 2π on the two separate peaks. However, this is not the case, as the ground state is decisively influencing the phase evolution on the excited state. It is also the reason why the occupancy does not vary at the excited state. In order to see this, let us keep in mind that, for example, the singlet Green

function is (up to a real positive coefficient) $1/(E_F - \epsilon_0 + 3J/4 + i\Gamma)$. At the triplet position, $\epsilon_0 = -J/4$, the value of the imaginary part of this Green function decays to $\Gamma/(\Gamma^2 + J^2)$, while the real part behaves as $J/(\Gamma^2 + J^2)$. Now, the real part of the triplet Green function itself, is zero at $\epsilon_0 = -J/4$ and has an evolution amplitude of the order $1/\Gamma$ on the resonance. If we multiply this with the peak height ratio, that is of the order Γ/J , we obtain the same magnitude as previously for the singlet contribution (in the limit of low Γ/J ratio).

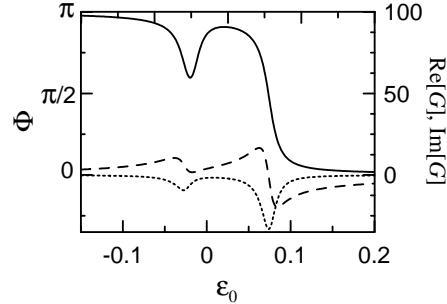


FIG. 3: Evolution of the phase Φ (solid curve), the real and the imaginary part of the single particle Green function $G = \langle\langle c_{0\sigma} | c_{0\sigma}^\dagger \rangle\rangle_{\omega=E_F}$ (dashed and dotted curves - in $1/D$ units) for the same parameters as in Fig.2a, upper panel.

The phase exactly at the triplet state is easy to calculate, and to observe a dip. One has to use the imaginary part of the triplet Green function and the real part of the singlet one (both calculated at the triplet position). We have some care in applying the arctan function: our intention is to visualize the real evolution of the phase, so we should compensate the artificial π drop from a definition of arctan (that happens at $\pi/2$); for angles greater than $\pi/2$ one should compute $\pi - \arctan$ for the value of the phase. In conclusion, we found, for small Γ/J , that the dip in the phase evolution reaches the value ($\pi - \arctan[6/\pi] \simeq 0.65\pi$) - see Fig.3. For the case of negative exchange parameter, and singlet excited state, the limit value for the dip would be ($\pi - \arctan[2/(3\pi)] \simeq 0.93\pi$). Fig.3 presents the phase evolution, the real and the imaginary part of the Green function. The plot should be read from right to left: the phase has a normal growing evolution on the peak corresponding to the ground state, then it presents a dip on the excited state peak. This dip is a signature of the excited states and can be used to probe the existence of such states through phase measurements. The phase evolution would be a much better method to detect excited states; it is more sensitive since it implies a ratio (of usually small quantities). Both dips in the phase evolution should be clearly seen experimentally, even when amplitude of the excited

state is too low to be noticed.

IV. KONDO REGIME

A study of the Kondo resonance requires a method, which takes into account correlations with electrons in the leads and the virtual spin-flip processes. One has to use the higher order decoupling scheme than that one used in the previous section. The next step of the EOM involves the Green functions with one operator from the leads and decoupling for the Green functions with two operators from the leads. Here, an example of the EOM equation

$$\begin{aligned}
(\omega - \epsilon_k) \langle \langle c_{0\uparrow} c_{0\downarrow}^\dagger c_{k\downarrow} S^z | c_{0\uparrow}^\dagger \rangle \rangle &= \langle c_{0\downarrow}^\dagger c_{k\downarrow} S^z \rangle + t \langle \langle c_{0\uparrow} c_{0\downarrow}^\dagger c_{0\downarrow} S^z | c_{0\uparrow}^\dagger \rangle \rangle + t \sum_q \langle \langle c_{q\uparrow} c_{0\downarrow}^\dagger c_{k\downarrow} S^z | c_{0\uparrow}^\dagger \rangle \rangle \\
&- t \sum_q \langle \langle c_{0\uparrow} c_{q\downarrow}^\dagger c_{k\downarrow} S^z | c_{0\uparrow}^\dagger \rangle \rangle + \frac{1}{4} J \langle \langle c_{0\uparrow} c_{0\downarrow}^\dagger c_{k\downarrow} | c_{0\uparrow}^\dagger \rangle \rangle + \frac{1}{4} J \langle \langle c_{k\downarrow} c_{0\downarrow}^\dagger c_{0\downarrow} S^- | c_{0\uparrow}^\dagger \rangle \rangle \\
&+ \frac{1}{4} J \langle \langle c_{k\downarrow} c_{0\uparrow}^\dagger c_{0\uparrow} S^- | c_{0\uparrow}^\dagger \rangle \rangle - \frac{1}{2} J \langle \langle c_{k\downarrow} c_{0\uparrow}^\dagger c_{0\uparrow} c_{0\downarrow}^\dagger c_{0\downarrow} S^- | c_{0\uparrow}^\dagger \rangle \rangle . \quad (12)
\end{aligned}$$

The higher order Green functions are decoupled according the following scheme

$$\begin{aligned}
\langle \langle c_{0\uparrow} c_{q\downarrow}^\dagger c_{k\downarrow} | c_{0\uparrow}^\dagger \rangle \rangle &\approx \langle c_{q\downarrow}^\dagger c_{k\downarrow} \rangle \langle \langle c_{0\uparrow} | c_{0\uparrow}^\dagger \rangle \rangle \approx \delta_{kq} f(\epsilon_k) \langle \langle c_{0\uparrow} | c_{0\uparrow}^\dagger \rangle \rangle , \quad (13) \\
\langle \langle c_{0\uparrow} c_{q\uparrow}^\dagger c_{k\downarrow} S^- | c_{0\uparrow}^\dagger \rangle \rangle &\approx \langle c_{q\uparrow}^\dagger c_{k\downarrow} S^- \rangle \langle \langle c_{0\uparrow} | c_{0\uparrow}^\dagger \rangle \rangle \approx \delta_{kq} \lambda f(\epsilon_k) \langle c_{0\uparrow}^\dagger c_{0\downarrow} S^- \rangle \langle \langle c_{0\uparrow} | c_{0\uparrow}^\dagger \rangle \rangle , \\
\langle \langle c_{0\uparrow} c_{q\downarrow}^\dagger c_{k\downarrow} S^z | c_{0\uparrow}^\dagger \rangle \rangle &\approx \delta_{kq} f(\epsilon_k) \langle \langle c_{0\uparrow} S^z | c_{0\uparrow}^\dagger \rangle \rangle + \delta_{kq} \lambda f(\epsilon_k) \langle c_{0\downarrow}^\dagger c_{0\downarrow} S^z \rangle \langle \langle c_{0\uparrow} | c_{0\uparrow}^\dagger \rangle \rangle .
\end{aligned}$$

The decoupling procedure follows the one first proposed by Meir[29] (also used e.g. in [18, 22, 30]) and, respectively, by Nagaoka [20] for the Green functions that also contain the localized spin operator. Like the cited papers, we considered that only the averages that conserve the total spin do not vanish. Further, one has to keep in mind, by examining the Hamiltonian (1), that exchange interaction between the leads electrons and the localized spin is only indirect and takes place through intermediate hopping on and off the QD. Supplementary from Nagaoka [20], and in order to keep the same level of complexity, we needed to approximate further the spin-spin average between the electrons in the leads and the localized spin; this was considered to be proportionate (by a factor λ) with the dot spin-spin correlator, multiplied with the probability of existence for the lead electron. It is reasonable to consider $\lambda < 1$, since the electrons in the leads are only indirectly coupled with the localized spin. We have checked that the main results are not qualitatively influence for any $\lambda < 1$. In our numerical calculations we put $\lambda = t^2/D^2$.

In this section, only the limit $U \rightarrow \infty$ and the Kondo regime will be considered (with the occupied level deep below E_F and the spin fluctuations not mixed with the charge fluctuations). This is the condition of strict validity for the decoupling scheme of Meir[29], some supplementary discussion on this aspect will be included in the end of the section (see also comments in [15]).

The solving procedure is as follows: first, the set of Eqs.(12) is solved (they are 14 in number), considering as parameters all the correlators. Due to the the decoupling scheme Eqs.(13), the set is now linear and can be solved. This is an important advantage of the decoupling that we have applied. The matrix that will need to be inversed in the system-solving algorithm has three (degenerate) eigenvalues: $1/(\omega - \epsilon_k)$, $1/(\omega - \epsilon_k + J)$ and $1/(\omega - \epsilon_k - J)$. Summing over k leads to appearance of three functions [23]

$$F_a(\omega) \equiv - \sum_k \frac{f(\epsilon_k)}{\omega - \epsilon_k + a} = i \frac{\pi}{2} + \ln \left(\frac{2\pi T}{D} \right) + \Psi \left(\frac{1}{2} - i \frac{\omega + a}{2\pi T} \right) \quad (14)$$

with $a = 0$ and $\pm J$. Here, Ψ denotes the digamma function. For $T < T_K$, the function F_a has a pronounced maximum around $\omega = -a$. Finally, we come back to the set of equations (5), which can now be solved.

Our model therefore predicts three peaks: one at the Fermi level $E_F = 0$ and two peaks symmetric on the left and right hand side, at $\pm J$, corresponding to the basic excitations in the system. Their position is given by the singlet-triplet energy distance similar to the case of an applied magnetic field [18]. The central peak can be associated to the fact that the triplet state by itself can develop such a Kondo resonance because it is three-fold degenerate. We point out than in the measurements of Sasaki (see Fig.4a in [14]) such a three-peak structure can be seen in the case of the triplet ground state and even for the singlet ground state, where the "zero" peak is however much less pronounced and the other two peaks are considerably enhanced.

We want to analyzed the Kondo resonance in the presence of a magnetic impurity, therefore we calculated the DOS for three cases: a) when both levels, singlet and triplet, are below E_F , b) the triplet state is below E_F , but the singlet state is above, and c) the singlet state is below E_F and the triplet above E_F . The results are in Fig.4. In the panel a), the singlet and triplet peaks overlap, due to the small J/Γ ratio. Such a small level spacing and increased coupling with the leads is exactly the case that allows the observation of three Kondo peaks in the DOS (a similar picture appears in measurements of the differential conductance). In

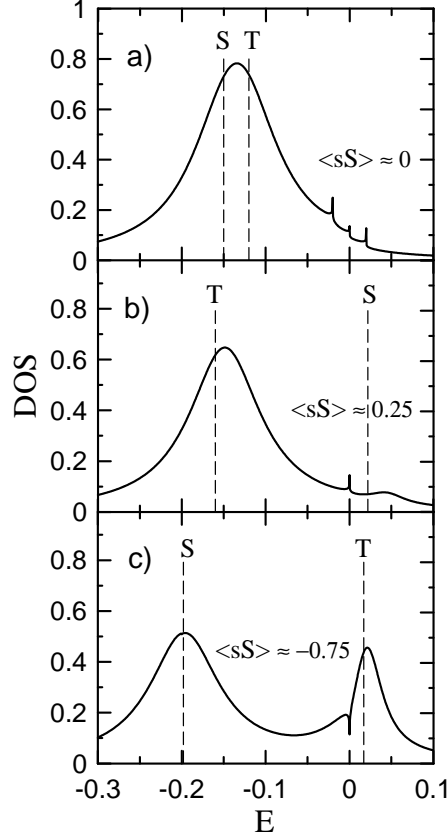


FIG. 4: Plots of the local density of states (DOS) for the Kondo regime: a) $\epsilon_0 = -0.15$ and $J = 0.02$; b) $\epsilon_0 = -0.11$ and $J = -0.2$; c) $\epsilon_0 = -0.05$ and $J = 0.2$. In plot a) we have a small exchange parameter and both singlet and triplet states are below $E_F = 0$. Three Kondo peaks appear at 0 and $\pm J$. In plot b) the exchange parameter has a large negative value and only the triplet state is below E_F , the Kondo resonance at 0 is present. In case c) with only the singlet state below E_F , the Kondo peak is no longer present. This can be related with the high negative value of the spin-spin correlator (the values are given in all graphs). Vertical lines indicate the position of the singlet and triplet levels. For all the three plots $\Gamma = 0.025$ and $T = 10^{-6}$.

this case, the correlation between the conduction electron in the dot and the localized spin is low $\langle \vec{s} \vec{S} \rangle \simeq 0$. This result is the same as obtained in the previous section, where we applied a perturbative decoupling, adapted for high temperatures case. That (more simple but analytical) calculation did not allow for the direct observation of the Kondo resonance. However, one could have made the prediction that the Kondo effect is allowed to develop, due to reduction of the spin-spin coupling. We believe the the experimental evidence [5] regarding the formation of the Kondo resonance (in the presence of magnetic impurities)

supports the result that the spin-spin correlator has reduced values when both singlet and triplet levels are below the Fermi energy.

For large level spacing (J), only the peak at E_F is of interest. This is similar to the case of a large applied magnetic field, or source-drain voltage, when the side peaks do not contribute to transport, and the Kondo effect is considered to disappear. Here a central peak is also present, and it remains important. Our calculations show that the Kondo peak is formed when the triplet state is below E_F (Fig4.b), and it does not form when only the singlet state is below E_F (Fig4.c). Such a result was expected from physical considerations, since the singlet state is not degenerate, and the Kondo effect only takes place for a degenerate up-most occupied level in the dot (it is not exclusively a spin effect, but, more generally, it originates in the Pauli exclusion principle).

In the following we will give an alternative explanation that relates the existence of the central Kondo peak with the value of the spin-spin correlator. In order to get a deeper insight on the formation of the Kondo resonances, one can assume that, in the vicinity the point $\omega = -a$, the function F_a (Eq.14) can be a dominating quantity in the Green function formula, and an expansion in $1/F_a$ can be done. To be more clear, we illustrate this idea first for the case $J = 0$, when we have the single-impurity Anderson Hamiltonian (within the approximations of Meir [29], which is similar to that of Lacroix' for high temperatures [15]). We have then

$$\langle\langle c_{0\uparrow}|c_{0\uparrow}^\dagger\rangle\rangle^{J=0} = \frac{1 - \langle n_{\bar{0}} \rangle}{\omega - \epsilon_0 + i\Gamma + t^2 F_0} \quad (15)$$

$$\frac{1}{\langle\langle c_{0\uparrow}|c_{0\uparrow}^\dagger\rangle\rangle^{J=0}} = t^2 \frac{1}{1 - \langle n_{\bar{0}} \rangle} F_0 + \dots \quad (16)$$

If the state ϵ_0 is deep below the Fermi level E_F , so $\langle n_{\bar{0}} \rangle \lesssim 0.5$, it results that the coefficient in front of F_0 in the expression for $1/\langle\langle c_{0\uparrow}|c_{0\uparrow}^\dagger\rangle\rangle$ is positive. It ensures the existence of the Kondo peak. If we look at the denominator of the Green function, we see that this is the condition for the " $\omega - \epsilon_0$ " line to intersect the logarithmical enhanced peak of F_0 , and to give therefore a peak in the density of states near E_F (see Fig.1 and Fig.2 in [15]). Of course, in the simple case $J = 0$, this is seen right away, the reason why we expressed the expansion of $1/\langle\langle c_{0\uparrow}|c_{0\uparrow}^\dagger\rangle\rangle$ is to compare the result with the same expansion for $J \neq 0$, when the analytical formula of $\langle\langle c_{0\uparrow}|c_{0\uparrow}^\dagger\rangle\rangle$ is much more complex and not so transparent (but the expansion that we mentioned gives a result easy to discuss).

In case of finite J we find

$$\frac{1}{\langle\langle c_{0\uparrow}|c_{0\uparrow}^\dagger\rangle\rangle} = t^2 \frac{1 - \frac{1}{3}\lambda\langle\vec{s}\vec{S}\rangle}{1 - \langle n_{\bar{0}} \rangle + \langle\vec{s}\vec{S}\rangle} F_0 + 0[\frac{1}{F_0}] \dots \quad (17)$$

The sign of the coefficient in front of F_0 depends on the sign of the denominator $1 - \langle n_{\bar{0}} \rangle + \langle\vec{s}\vec{S}\rangle$, because the numerator is always positive. In the Kondo regime, we have $\langle n_{\bar{0}} \rangle \approx 0.5$ and the denominator changes its sign for $\langle\vec{s}\vec{S}\rangle$. Three cases are presented in Fig.4: the case a) with $\langle\vec{s}\vec{S}\rangle \simeq 0$, b) $\langle\vec{s}\vec{S}\rangle \simeq 1/4$, and the case c) with $\langle\vec{s}\vec{S}\rangle \simeq -3/4$. For the case a) the coefficient in front of F_0 in the expansion (17) is positive, and DOS shows the peak at E_F . In the case b), when the triplet is below E_F and singlet above E_F , the spin-spin average is positive (with a maximum value $1/4$), as the triplet state favors ferromagnetic coupling. For this case again the coefficient in front of F_0 is positive. A different situation is encountered in case c), when singlet is below E_F and triplet is above E_F . The spin-spin average is negative and, for large J , it can reach the minimal value $-3/4$. In this case the coefficient of F_0 is negative, preventing the formation of the Kondo resonance.

According to our calculations, the Kondo effect develops for $\langle\vec{s}\vec{S}\rangle > -0.5$. Our calculations indicate also a possible quantitative estimation about the influence of the spin-spin correlator on the formation of the Kondo resonance.

In this section we have focused exclusively on the description of the Kondo peaks. The plots in Fig.4, are for DOS, and not for the conductance, that is of course the measurable quantity. However, it is known that the differential conductance (the main experimental tool used in such cases) accurately follows the DOS, so it is not necessary to repeat the plots.

On the other hand, for the description of both charge and spin fluctuations (and the mixed valence regime), one encounters the case when the energy levels of the dot become $\epsilon_0 \simeq E_F$, which is outside the Kondo regime, and the decouplings of Meir are no longer reliable. This is the limitation of the Meir approach, that on the other hand has the advantage of allowing for a clear insight on the the Kondo regime of complex systems. For the mixed-valance regime, the approximation made by Lacroix [15] for the single impurity Anderson model, at low temperatures, should be used instead. This is still possible for systems with a complex noninteracting network around the impurity [16, 17, 31, 32, 33]. But when interaction terms are added, like the problem we address in the present paper, great technical difficulties appear. This justifies the complementary use of the more simple decoupling scheme made in

the previous section, that can be interpreted as a second order perturbation in respect with the coupling and allows to address all parameters range (but does not capture the Kondo effect).

V. CONCLUSIONS

The paper addresses the problem of electronic transport through a quantum dot with a magnetic impurity. The exchange interaction between the impurity spin and the spin of the conduction electron in the dot generates a singlet-triplet splitting of the spectrum.

Using the EOM technique, we gave a detailed presentation of the solving procedure, which takes into account all the electronic correlations in the dot - both in high and low temperatures regimes. For temperatures higher than T_K , analytical solutions were found which were exploited to obtain a detailed description of the evolution of the spin-spin correlator, the height of the conductance peaks, and the phase evolution. The evolution of the spin-spin coupling is found to have low values when both singlet and triplet levels are below the Fermi energy, when the total magnetic moment approaches the value for two free electrons; such a situation is favorable for the developing of the Kondo effect, once the temperature is lowered (and a more accurate decoupling scheme is applied).

A formula is given for the singlet/triplet peak height ratio, showing that the ground state is usually much better seen in transport than the excited state, no matter if it is singlet or triplet (depending on the sign of J ; this differs from the constant $1/3$ ratio from the two-electrons spin-scattering picture, when the Fermi sea is neglected). For low J/Γ (exchange versus coupling) ratio, the excited states are very weakly seen in transport but the phase of the single electron Green function still presents a specific dip (of considerable amplitude) at the excited state position, and could be experimentally used for the detection of such states.

For low temperatures, we find three Kondo peaks: one at E_F and the other two at $E_F \pm J$, corresponding to the basic excitation energy. For large values of the exchange parameter, it is possible that only one state (either triplet or singlet) is below E_F . In the case when only the singlet state is below E_F , the Kondo peak at E_F does not form (and it does form in the case of the triplet below E_F). This is due to the fact that antiferromagnetic coupling suppresses the Kondo effect, but also because the Kondo effect needs a degenerate up-most occupied level in the dot. We proved this in a transparent way, making the connection with

the value of the spin-spin correlator.

Acknowledgments

The work was supported by the project RTNNANO contract No. MRTN-CT-2003-504574 and in part by the Ministry of Science and Information Society Technologies.

APPENDIX A: SPECTRUM OF THE ISOLATED DOT

The isolated dot is described by the Hamiltonian (1) if we put $t = 0$. The energy spectrum is for empty state, with one and two electrons at the state ϵ_0 . The empty state energy we have chosen *zero* by convention. For single occupancy we have

$$\begin{aligned}
 H|\uparrow\uparrow\rangle &= (\epsilon_0 + \frac{1}{4}J)|\uparrow\uparrow\rangle \quad (\text{Triplet}) \\
 H|\downarrow\downarrow\rangle &= (\epsilon_0 + \frac{1}{4}J)|\downarrow\downarrow\rangle \quad (\text{Triplet}) \\
 H\frac{1}{\sqrt{2}}(|\uparrow\downarrow\rangle + |\downarrow\uparrow\rangle) &= (\epsilon_0 + \frac{1}{4}J)\frac{1}{\sqrt{2}}(|\uparrow\downarrow\rangle + |\downarrow\uparrow\rangle) \quad (\text{Triplet}) \\
 H\frac{1}{\sqrt{2}}(|\uparrow\downarrow\rangle - |\downarrow\uparrow\rangle) &= (\epsilon_0 - \frac{3}{4}J)\frac{1}{\sqrt{2}}(|\uparrow\downarrow\rangle - |\downarrow\uparrow\rangle) \quad (\text{Singlet})
 \end{aligned} \tag{A1}$$

where $|\uparrow\uparrow\rangle$ is the state with the electron with the spin $\sigma = \uparrow$ at the state ϵ_0 and the spin up at the impurity, etc.

For double occupancy, we have a two-fold degenerate state

$$\begin{aligned}
 H|\uparrow\downarrow\uparrow\rangle &= (2\epsilon_0 + U)|\uparrow\downarrow\uparrow\rangle \\
 H|\uparrow\downarrow\downarrow\rangle &= (2\epsilon_0 + U)|\uparrow\downarrow\downarrow\rangle
 \end{aligned} \tag{A2}$$

For single occupancy, we see that there are two possible states. The lowest in energy will be the ground state of the system (singlet for positive J and triplet for negative J), and the other will be excited state. The resonances of the system are found with the condition $E(n) = E(n + 1)$, where n is the number of electrons in the system. For the adding of the first electron we have the resonances at $\epsilon_0 = 3J/4$ and $\epsilon_0 = -J/4$; for the adding of the

second electron we will have two resonances at $\epsilon_0 = -U + J/4$ and $\epsilon_0 = -U - 3J/4$.

- [1] T. Dietl, H. Ohno, F. Mtsukura, J. Cibert, and D. Ferrand, *Science* **287**, 1019 (2000).
- [2] A.O. Govorov, *Phys. Rev. B* **70**, 035321 (2004).
- [3] G.Murthy, *Phys. Rev. Lett.* **94**, 126803 (2005).
- [4] A.Aldea, M. Tolea, J. Zittartz, *Physica E* **28**, 191 (2005).
- [5] H. B. Heersche,Z. de Groot, J. A. Folk, L. P. Kouwenhoven, H. S. J. van der Zant, A.A. Houck, J. Labaziewicz, I.L. Chuang *Phys. Rev. Lett.* **96**, 017205 (2006).
- [6] N.J. Craig, J.M. Taylor, E.A. Lester, C.M. Marcus, M.P. Hanson, and A.C. Gossard, *Science* **304**, 565 (2004).
- [7] P. Simon, R. López, and Y. Oreg, *Phys. Rev. Lett.* **94**, 086602 (2005).
- [8] M.G. Vavilov and L.I. Glazman, *Phys. Rev. Lett.* **94**, 086805 (2005).
- [9] D. Goldhaber-Gordon, Hadas Shtrikman, D. Mahalu, David Abusch-Magder, U. Meirav and M. A. Kastner, *Nature* **391**, 156 (1998) .
- [10] S. M. Cronenwett, T. H. Oosterkamp, and L. P. Kouwenhoven, *Science* **281** (1998) 540.
- [11] T. Rejec, A. Ramsak, and J.H. Jefferson, *Phys. Rev. B* **67**, 075311 (2003).
- [12] B. R. Bulka and T. Kostyrko, *Phys. Rev. B* **70**, 205333 (2004).
- [13] T. Kostyrko and B. R. Bulka, *Phys. Rev. B* **71**, 235306 (2005).
- [14] S. Sasaki, S. De Franceschi, J.M Elzerman, W.G. van der Wiel, M. Eto, S. Tarucha and L.P. Kouwenhoven, *Nature* **405**, 764 (2000).
- [15] C. Lacroix, *J. Phys. F: Metal Phys.* **11**, 2389 (1981).
- [16] B. R. Bulka and P. Stefański, *Phys. Rev. Lett.* **86**, 5128 (2001).
- [17] O. Entin-Wohlman, A. Aharony, and Y. Meir, *Phys. Rev. B* **71**, 035333 (2005).
- [18] Y. Meir, N.S. Wingreen, P.A. Lee *Phys. Rev. Lett.* **70**, 2601 (1993).
- [19] Y.Meir, N.S. Wingreen, *Phys. Rev. Lett.* **68** 2512 (1992).
- [20] Y. Nagaoka, *Phys. Rev.* **138**, A1112 (1965).
- [21] A. Theumann, *Phys. Rev.* **178**, 978 (1968).
- [22] P. Zhang, Q.-K. Xue, Y.P. Wang, and X.C. Xie, *Phys. Rev. Lett.* **89**, 286803 (2002).
- [23] D.R. Hamann, *Phys. Rev* **158**, 570 (1967).
- [24] M.C. Rogge, B. Harke, C. Fricke, F. Hohls, M. Reinwald, W. Wegscheider, and R.J. Haug,

Phys. Rev. B **72**, 233402 (2005).

[25] L. D. Landau and E. M. Lifshitz, *Quantum Mechanics*, Pergamon, Oxford, 1977; J. R. Oppenheimer, Phys. Rev. **32**, 361 (1928); N. F. Mott, Proc. R. Soc. London, Ser. A **126**, 259 (1930).

[26] G. Hackenbroich, Phys. Rep. **343**, 463 (2001).

[27] R. Schuster, E. Buks, M. Heiblum, D. Mahalu, V. Umansky, H. Shtrikman, Nature **385**, 417 (1997).

[28] A. Yacoby, M. Heiblum, D. Mahalu, H. Shtrikman, Phys. Rev. Lett. **74**, 4047 (1995).

[29] Y. Meir, N. S. Wingreen and P. A. Lee, Phys. Rev. Lett. **66**, 3048 (1991).

[30] Q.-F. Sun and H. Guo, Phys. Rev. B **64**, 153306(R) (2001).

[31] W. Hofstetter, J. König, and H. Schoeller, Phys. Rev. Lett. **87**, 156803 (2001).

[32] P. Stefanski, A. Tagliacozzo, and B. R. Bulka Phys. Rev. Lett. **93**, 186805 (2004).

[33] P. Stefański, Solid State Comm. **128**, 29 (2003). .